Detailed rate coefficients and the enthalpy change of the equilibrium reaction OH+C2H4=MHOC2H4 over the temperature range 544–673 K

Eric WeiGuang Diau and YuanPern Lee

Citation: The Journal of Chemical Physics **96**, 377 (1992); doi: 10.1063/1.462474
View online: http://dx.doi.org/10.1063/1.462474
View Table of Contents: http://scitation.aip.org/content/aip/journal/jcp/96/1?ver=pdfcov
Published by the AIP Publishing

Detailed rate coefficients and the enthalpy change of the equilibrium reaction $OH + C_2H_4 \overset{M}{\rightleftharpoons} HOC_2H_4$ over the temperature range 544–673 K

Eric Wei-Guang Diau and Yuan-Pern Lee[a)]
Department of Chemistry, National Tsing Hua University, 101, Sec. 2, Kuang Fu Road, Hsinchu, Taiwan 30043, Republic of China

(Received 8 July 1991; accepted 23 September 1991)

The reaction between OH and C_2H_4 in He has been studied over the pressure range 278–616 Torr and the temperature range 544–673 K by means of the laser-photolysis/laser-induced-fluorescence technique. Analysis of the temporal profile of [OH] yielded the equilibrium constant for the reaction $OH + C_2H_4 + M \rightleftharpoons HOC_2H_4 + M$. The temperature dependence of the equilibrium constant led to the enthalpy of reaction $\Delta H = -(30.3 \pm 0.8)$ kcal mol^{-1} and the entropy of reaction $\Delta S = -(30.9 \pm 1.0)$ cal K^{-1} mol^{-1} near 600 K, in agreement with previous predictions. Analysis of the detailed rate coefficients suggests that the H-atom abstraction reaction is relatively unimportant in the temperature range of our study; the rate coefficient determined previously for the H-atom abstraction near 673 K may have been overestimated. The temperature dependence of the rate coefficients for the forward, the reverse, and the adduct-loss reactions have been determined to be $k_f = (4 \pm 3) \times 10^{-13} \exp[(1200 \pm 800)/T]$ cm^3 molecule^{-1} s^{-1}, $k_r = (6.2 \pm 1.0) \times 10^{11} \exp[-(11\,900 \pm 400)/T]$ s^{-1}, and $k_a = (8.8^{+25}_{-1.5}) \times 10^9 \exp[-(10\,400^{+1600}_{-400})/T]$ s^{-1}, respectively.

I. INTRODUCTION

The reaction of OH with C_2H_4 is important in the combustion of hydrocarbons[1,2] as well as in atmospheric chemistry.[3,4] There have been numerous experimental investigations of the rate coefficient and the mechanism of this reaction,[5–30] and reviews of the results.[31–33] At low temperatures ($T < 500$ K), the initial step of the reaction is dominated by the electrophilic addition of OH to C_2H_4 to form an adduct $HOC_2H_4^*$, followed by decomposition, stabilization, or isomerization of this adduct

$$OH + C_2H_4 \rightleftharpoons HOC_2H_4^*, \quad (1,-1)$$

$$HOC_2H_4^* + M \rightarrow HOC_2H_4 + M, \quad (2)$$

$$HOC_2H_4^* \rightarrow \text{isomerization/decomposition products.} \quad (3)$$

The rate coefficient was generally determined by monitoring the consumption of OH. It depends on pressure and, at the high pressure limit, decreases slightly as temperature increases. In the temperature range 500–750 K, the rate coefficient decreases more rapidly as temperature increases; this is because the decomposition of the thermalized HOC_2H_4 back to OH and C_2H_4,

$$HOC_2H_4 + M \rightarrow HOC_2H_4^* + M, \quad (-2)$$

$$HOC_2H_4^* \rightarrow OH + C_2H_4, \quad (-1)$$

becomes important in this temperature range. At high temperatures ($T > 750$ K), the abstraction of an H atom

$$OH + C_2H_4 \rightarrow H_2O + C_2H_3 \quad (4)$$

becomes the major channel and the rate coefficient increases rapidly as the temperature increases.

Few spectroscopic studies of the HOC_2H_4 adduct have been reported. The electron-spin resonance (ESR) spectrum of HOC_2H_4 recorded in the photolysis of ethanol containing 1% H_2O_2 at -70 °C[34,35] and in the reduction of $HOCH_2CH_2I$[36] suggested the nonequivalence of the α and/or β protons. In a recent experiment using the pulse-radiolysis/kinetic-absorption technique, a structureless UV absorption in the range 210–265 nm was attributed to HOC_2H_4; the self-reaction of HOC_2H_4 was also studied.[37] No infrared spectrum of HOC_2H_4 has been reported. Theoretical calculations have been performed to predict the structure of HOC_2H_4 and the barrier heights and the structures of intermediates in various paths of the isomerization and decomposition of HOC_2H_4.[38–40] The enthalpy change for the title reaction has not been determined experimentally. According to empirical estimates, ΔH^0 is in the range $-(29–35)$ kcal mol^{-1},[17,24,29,41,42] whereas *ab initio* calculations[38–40] gave values of $-(24–29)$ kcal mol^{-1}.

We have investigated the title reaction at temperatures ranging from 544 to 673 K by means of the laser-photolysis/laser-induced-fluorescence (LIF) technique. Through a careful control of experimental parameters to achieve equilibrium conditions suitable for an accurate determination of the double-exponential decay of [OH], we have been able to determine the equilibrium constant and the detailed rate coefficients of the title reaction. The temperature dependence of the equilibrium constant yields ΔH and ΔS of the reaction.

II. EXPERIMENTAL

The technique and the experimental setup have been described in detail previously,[43] hence only a summary is

[a)] Also affiliated with the Institute of Atomic and Molecular Sciences, Academia Sinica, Taiwan, Republic of China.

 0021-9606/92/010377-10$06.00

given here. A few modifications have been made in order to carry out the reaction at high temperature.

The quartz reaction cell wrapped with the Nichrome heater and heat insulator was resistively heated to the desired temperature. A temperature controller (Omega model CN9000) monitored the output of a type K thermocouple (inserted slightly above the laser-probed reaction zone) and regulated the temperature of the cell to ± 2 °C. The thermocouple was calibrated to ± 1 °C. In a few experiments, the temperature of the reactants was also derived from the intensity distribution of various rotational lines in the laser excitation spectrum of OH; consistent results were obtained. The uniformity of the temperature in the reaction zone was checked by moving the thermocouple along the probed volume; the deviation was determined to be less than 1%.

Because HNO_3 and H_2O_2 decompose at high temperature, an alternative source of OH was used. The OH radicals were generated by photolysis of N_2O with an ArF laser (193 nm, 3–10 mJ cm^{-2}) to give $O(^1D)$ and N_2,

$$N_2O \overset{193\ nm}{\rightarrow} N_2 + O(^1D) \tag{5}$$

followed by the rapid reaction of $O(^1D)$ with H_2O,

$$O(^1D) + H_2O \rightarrow OH + OH, \tag{6}$$

in which $k_6 = 2.2\times10^{-10}$ cm^3 $molecule^{-1}$ s^{-1}.[32] Because the temporal profile of [OH] was monitored normally in the reaction period 50 μs–10 ms, a relatively large concentration of H_2O ($\sim 5\times10^{15}$ molecules cm^{-3}) was added in order to convert most $O(^1D)$ into OH within 5 μs after photolysis.

The relative concentration of OH was determined from the gated integrated fluorescence intensity of OH which was excited by a probe laser at a varied delay after the photolysis laser. The probe laser was a frequency-doubled dye laser pumped by the 532 nm emission of a Nd-YAG laser. The excitation wavelength of OH was 282.0 nm and the fluorescence near 310 nm was detected. The repetition rates of both lasers were set at 10 Hz and the fluorescence signal was typically averaged over 100 pulses at each delay.

All experiments were carried out under slow flow conditions so as to replenish the reactants. The diluent gas He (99.9995%) was used without further purification. N_2O (99%) was degassed at 165 K before used. A diluted gas sample of C_2H_4 (1.75% $\pm$ 0.07% in He) prepared with standard gas-handling techniques was used in the experiments. The concentration of the C_2H_4/He mixture was determined by comparison of the integrated IR absorption (resolution 1 cm^{-1}) to those samples with known concentration.

Typical experimental conditions were as follows: total flow rate $F_T = 7 - 16$ STP cm^3 s^{-1} (STP = 1 atm and 273 K); total pressure $P = 278$–616 Torr; reaction temperature $T = 544$–673 K; flow velocity $\bar{v} \simeq 2$–5 cm s^{-1}; $[H_2O] \simeq (4$–$7)\times10^{15}$ molecules cm^{-3}; $[N_2O] \simeq (0.2$–$2.0)\times10^{15}$ molecules cm^{-3}; $[C_2H_4] \simeq (2.4$–$199.8)\times10^{14}$ molecules cm^{-3}; $[OH]_0 \simeq (1$–$4)\times10^{11}$ molecules cm^{-3}; the interval between the photolysis laser and the probe laser is $t = 20\,\mu$s–30 ms.

III. RESULTS AND DISCUSSION

Photolysis of N_2O with the ArF laser produced $O(^1D)$ almost instantly. However, the reaction of $O(^1D)$ with H_2O required a few microseconds for completion. The OH radicals were produced rapidly, reached their maximum concentration in less than 5 μs, and decayed slowly afterwards. A simplified mechanism consisting of the following reactions:

$$O(^1D) + H_2O \rightarrow OH + OH, \tag{6}$$

$$O(^1D) \overset{M}{\rightarrow} O(^3P), \tag{7}$$

$$OH \rightarrow \text{loss} \tag{8}$$

was used to model the production of OH. Reaction (7) includes all possible $O(^1D)$-depletion reactions other than reaction (6). The temporal profile of OH was derived by solution of the differential rate equations for reactions (6)–(8)

$$[OH] = 2k_6[H_2O][O(^1D)]_0\,[\exp(-k_8 t) - \exp(-k_q t)]/(k_q - k_8), \tag{9}$$

in which

$$k_q = k_6[H_2O] + k_7 \tag{10}$$

and $[O(^1D)]_0$ is the initial concentration of $O(^1D)$ after photolysis. Provided that $k_q \gg k_8$, the maximum concentration of OH is expressed by the equation

$$[OH]_{max} = 2k_6[H_2O][O(^1D)]_0/k_q. \tag{11}$$

Typically k_q was adjusted to exceed 1×10^6 s^{-1} so that $[OH]_{max}$ was reached within 10 μs after photolysis; hence $[OH]_{max}$ was taken as $[OH]_0$, the 'initial' [OH] before its reaction with C_2H_4. The decay rate of OH, k_8, was normally in the range 20–80 s^{-1}.

The title reaction was then carried out with $[C_2H_4] \gg [OH]_0$ in the reaction cell. In Fig. 1, typical temporal profiles of [OH] at various concentrations of C_2H_4 at 575 K are shown. The double-exponential character was not evident in the temporal profile of [OH] with smaller

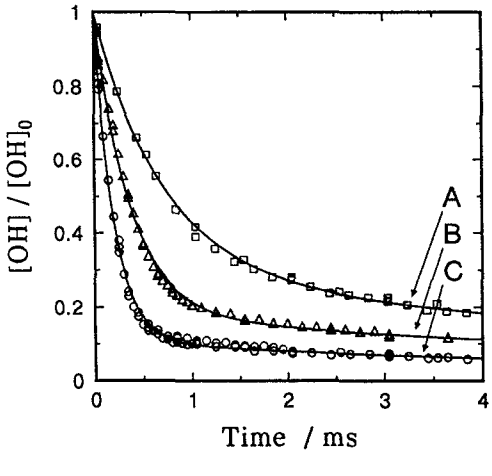

FIG. 1. Temporal profiles of [OH] at 286 Torr and 575 K. $[OH]_0 \simeq 1\times10^{11}$ molecules cm^{-3}, $[C_2H_4]$ (10^{15} molecules cm^{-3}) = (A) 0.65; (B) 1.27; (C) 2.36. The solid curves represent the nonlinear least-squares fit.

$[C_2H_4]$ (trace A); data of such decay characteristics were not used. Traces B and C, obtained with greater $[C_2H_4]$, exhibited distinctly double-exponential decays with a rapid decay toward the equilibrium concentration within 1 ms of reaction period followed by a much slower decay in the millisecond range. An increase in $[C_2H_4]$ decreased [OH] more rapidly and resulted in a smaller $[OH]/[OH]_0$ ratio throughout the entire decay.

A simplified mechanism consisting of reactions (6), (7), and

$$OH + C_2H_4 \xrightarrow{M} HOC_2H_4, \tag{12f}$$

$$HOC_2H_4 \xrightarrow{M} OH + C_2H_4, \tag{13r}$$

$$HOC_2H_4 \rightarrow \text{products other than OH}, \tag{14a}$$

$$OH \rightarrow \text{products other than } HOC_2H_4 \tag{15}$$

was used to model the reactions. For clarity, the rate coefficients of reactions (12)–(14) are expressed as k_f (the effective second-order rate coefficient for the forward reaction), k_r (the effective first-order rate coefficient for the reverse reaction), and k_a (the effective first-order rate coefficient for the reaction of the adduct), respectively. Reaction (14) includes the possible isomerization and decomposition processes of HOC_2H_4 other than reaction (13), as well as the diffusion of HOC_2H_4 from the probed volume. Reaction (15) is an extension of reaction (8); it takes into account reaction (4) (the H-atom abstraction channel), all possible reactions of OH with species other than C_2H_4, and the diffusion of OH away from the probed volume. To the first approximation,

$$k_{15} \simeq k_4[C_2H_4] + k_8. \tag{16}$$

We derived the temporal profile of [OH] in the presence of C_2H_4 by solving the differential rate equations for reactions (6), (7), and (12)–(15) to yield

$$[OH] = 2k_6[H_2O][O(^1D)]_0 \left[\frac{(\gamma - k_q)\exp(-k_q t)}{(k_q-\lambda_1)(k_q-\lambda_2)} + \frac{(\gamma-\lambda_1)\exp(-\lambda_1 t)}{(k_q-\lambda_1)(\lambda_2-\lambda_1)} - \frac{(\gamma-\lambda_2)\exp(-\lambda_2 t)}{(k_q-\lambda_2)(\lambda_2-\lambda_1)}\right], \tag{17}$$

in which

$$\lambda_1 = [\alpha - (\alpha^2 - 4\beta)^{1/2}]/2 > 0, \tag{18}$$

$$\lambda_2 = [\alpha + (\alpha^2 - 4\beta)^{1/2}]/2 > \lambda_1 > 0, \tag{19}$$

$$\gamma = k_r + k_a, \tag{20}$$

$$\alpha = k_f[C_2H_4] + k_r + k_a + k_{15}, \tag{21}$$

$$\beta = k_f k_a[C_2H_4] + k_r k_{15} + k_a k_{15}. \tag{22}$$

Provided that $k_q \gg \lambda_2 \gg \lambda_1$, the initial rise of [OH] is taken as instantaneous and the expression for [OH] is simplified to

$$[OH] = [OH]_0[(\gamma-\lambda_1)\exp(-\lambda_1 t) - (\gamma-\lambda_2)\exp(-\lambda_2 t)]/(\lambda_2-\lambda_1). \tag{23}$$

Equation (23) is identical to that derived previously[43] from a four-step mechanism for the reaction of $OH + CS_2$ in which OH was produced directly from photolysis of HNO_3 or H_2O_2. Because data points with a reaction period less than 50 μs were generally not used, the rise of [OH] did not interfere in the fitting of the temporal profile to a double-exponential decay of [OH].

In order to obtain accurate values of the parameters λ_1, λ_2, and γ from the least-squares fit of the [OH] temporal profile using Eq. (23), we adjusted the experimental conditions so that a distinctly double-exponential decay profile of [OH] was observed (i.e., $\alpha^2 \gg \beta$, which also implies that $\lambda_2 \simeq \alpha \gg \lambda_1 \simeq \beta/\alpha$). Under such conditions, the reactions may be taken as a two-step process—a rapid approach to equilibrium and a slow decay after the equilibrium is reached. The component of the slow decay is expressed as

$$[OH] = [OH]_0(\gamma-\lambda_1)\exp(-\lambda_1 t)/(\lambda_2-\lambda_1) = [OH]_{eq}\exp(-\lambda_1 t). \tag{24}$$

If the equilibrium concentration of OH, $[OH]_{eq}$, was not too small, λ_1 could be determined accurately. At lower temperatures, the forward reaction is much more rapid than the reverse reaction; hence the equilibrium constant K_c becomes greater

$$K_c = k_f/k_r = [HOC_2H_4]_{eq}/[OH]_{eq}[C_2H_4]_{eq}. \tag{25}$$

In order to maintain a suitable value of $[OH]_{eq}$ for accurate measurements of rate coefficients, we decreased the initial concentration of C_2H_4. However, the decrease in $[C_2H_4]$ reduces α^2 more rapidly than β; consequently, the condition $\lambda_2 \gg \lambda_1$ does not hold for small $[C_2H_4]$. At higher temperatures, the rate of the reverse reaction becomes greater, hence large $[C_2H_4]$ was used in order to maintain a reasonable $[OH]_{eq}$. However, at $T > 673$ K, we found it difficult to maintain the condition $\lambda_2 \gg \lambda_1$ because the rate coefficients of the loss of HOC_2H_4 and OH, k_r, k_a, and k_{15} increased rapidly at higher temperature. Therefore, temporal profiles of [OH] with distinctly double-exponential decay could be obtained within only limited ranges of temperature, pressure, and $[C_2H_4]$.

The observed temporal profiles of [OH] were fitted to Eq. (23) by means of a nonlinear least-squares method to determine λ_1, λ_2, and γ. The values of α and β were then derived from λ_1 and λ_2 according to Eqs. (18) and (19). The determined values of α, β, γ, and the experimental conditions are all listed in Tables I and II.

It is difficult to derive individual rate coefficient accurately without the knowledge of either k_a or k_{15}. As described previously,[43] for the temporal profiles with distinctly double-exponential behavior, a simple method was used to determine the equilibrium constant without an explicit solution of k_f and k_r. If the fraction of unreacted OH when the equilibrium was reached is expressed as x_{eq}, from Eq. (24)

$$x_{eq} = [OH]_{eq}/[OH]_0 = (\gamma-\lambda_1)/(\lambda_2-\lambda_1). \tag{26}$$

If one assumes that reactions (14) and (15) were negligible when the equilibrium was reached under our experimental conditions,

$$[HOC_2H_4]_{eq} = [OH]_0 - [OH]_{eq}. \tag{27}$$

Accordingly, the equilibrium constant K_c becomes

TABLE I. A summary of experimental conditions and fitted decay parameters of the temporal profile of [OH] at $544 < T < 595$ K.[a]

Expt. no.	T (K)	P (Torr)	$[C_2H_4]$ (10^{13})[b]	$[N_2O]$ (10^{13})[b]	$[H_2O]$ (10^{14})[b]	α $(10^3\ s^{-1})$	β $(10^5\ s^{-2})$	γ $(10^2\ s^{-1})$	x_{eq} (10^{-2})	K_p $(10^4\ atm^{-1})$
1	544	387	23.5	220	62	0.95 ± 0.02	0.34 ± 0.07	1.73 ± 0.16	15.5 ± 2.0	31.36 ± 5.14
2		384	36.8			1.50 ± 0.02	0.58 ± 0.11	1.93 ± 0.16	10.8 ± 1.2	30.13 ± 4.15
3	550	613	37.8	16	70	1.62 ± 0.02	1.02 ± 0.08	2.74 ± 0.13	14.0 ± 1.0	21.64 ± 2.07
4	558	384	29.8	215	60	1.27 ± 0.02	0.85 ± 0.05	3.67 ± 0.15	26.2 ± 1.5	12.40 ± 1.13
5		385	52.4			2.04 ± 0.03	1.44 ± 0.10	3.91 ± 0.16	16.8 ± 0.9	12.43 ± 1.00
6			100.7			3.61 ± 0.07	2.49 ± 0.57	4.21 ± 0.36	10.1 ± 1.1	11.59 ± 1.57
7	566	610	47.7	150	68	1.92 ± 0.04	1.80 ± 0.09	5.40 ± 0.22	25.6 ± 1.4	7.88 ± 0.69
8		612	75.0			3.11 ± 0.05	2.89 ± 0.25	5.49 ± 0.26	15.5 ± 1.0	9.39 ± 0.83
9		611	93.1			3.64 ± 0.04	3.57 ± 0.23	5.47 ± 0.20	13.0 ± 0.6	9.35 ± 0.71
10	573	537	40.5	83	53	1.78 ± 0.04	1.51 ± 0.05	7.19 ± 0.23	39.4 ± 1.7	4.88 ± 0.42
11		539	73.4			2.76 ± 0.05	2.57 ± 0.13	7.66 ± 0.29	26.1 ± 1.2	4.95 ± 0.40
12	572	539	107.2			4.18 ± 0.07	3.90 ± 0.23	7.87 ± 0.28	17.4 ± 0.8	5.70 ± 0.42
13	575	286	126.6			2.83 ± 0.05	3.22 ± 0.20	5.87 ± 0.26	18.0 ± 1.1	4.58 ± 0.40
14	575	290	163.3			3.73 ± 0.04	4.28 ± 0.26	6.15 ± 0.22	14.2 ± 0.7	4.72 ± 0.35
15	573	278	169.2			3.43 ± 0.10	4.39 ± 0.54	6.02 ± 0.48	14.8 ± 1.7	4.35 ± 0.61
16	575	286	236.2			5.17 ± 0.07	7.00 ± 0.68	6.61 ± 0.32	10.7 ± 0.7	4.52 ± 0.41
17	581	613	66.2	140	66	2.94 ± 0.06	3.98 ± 0.21	9.22 ± 0.38	29.3 ± 1.6	4.59 ± 0.42
18		614	101.3			4.38 ± 0.06	6.17 ± 0.30	9.56 ± 0.29	19.8 ± 0.8	5.04 ± 0.35
19	590	614	79.1	138	65	3.82 ± 0.06	6.09 ± 0.15	13.02 ± 0.30	32.6 ± 1.0	3.26 ± 0.22
20		615	123.6			4.54 ± 0.13	7.29 ± 0.59	11.45 ± 0.64	23.2 ± 1.7	3.33 ± 0.35
21			165.1			5.91 ± 0.14	9.43 ± 0.79	11.51 ± 0.59	17.7 ± 1.2	3.51 ± 0.33
22	593	380	71.6	202	62	2.83 ± 0.08	4.28 ± 0.20	12.60 ± 0.56	43.9 ± 2.6	2.21 ± 0.26
23	595	386	101.5			3.71 ± 0.07	5.34 ± 0.21	14.21 ± 0.43	37.2 ± 1.5	2.05 ± 0.16
24	594	382	128.8			4.82 ± 0.07	7.77 ± 0.28	14.18 ± 0.35	27.9 ± 0.9	2.48 ± 0.17
25	593	386	192.9			6.49 ± 0.11	9.97 ± 0.57	14.19 ± 0.45	20.4 ± 0.8	2.50 ± 0.18

[a]The uncertainties represent one standard deviation.
[b]In units of molecules cm^{-3}.

TABLE II. A summary of experimental conditions and fitted decay parameters of the temporal profile of [OH] at $603 < T < 673$ K.[a]

Expt. no.	T (K)	P (Torr)	$[C_2H_4]$ (10^{13})[b]	$[N_2O]$ (10^{13})[b]	$[H_2O]$ (10^{14})[b]	α $(10^3\ s^{-1})$	β $(10^5\ s^{-2})$	γ $(10^2\ s^{-1})$	x_{eq} (10^{-2})	K_p $(10^4\ atm^{-1})$
26	603	616	191.5	140	63	6.62 ± 0.15	14.27 ± 0.52	24.35 ± 0.76	35.8 ± 1.5	1.14 ± 0.09
27		320	99.9	73	56	3.79 ± 0.10	8.10 ± 0.33	15.67 ± 0.63	40.2 ± 2.2	1.81 ± 0.19
28		322	166.7			5.36 ± 0.12	11.41 ± 0.64	16.16 ± 0.66	28.4 ± 1.5	1.85 ± 0.17
29		316	251.3			6.07 ± 0.11	12.89 ± 0.59	16.52 ± 0.53	25.4 ± 1.0	1.42 ± 0.11
30		320	517.3			11.29 ± 0.15	28.85 ± 1.65	18.12 ± 0.57	14.4 ± 0.6	1.40 ± 0.10
31	613	411	109.6	38	72	4.08 ± 0.14	8.66 ± 0.38	23.94 ± 0.97	54.2 ± 3.2	0.924 ± 0.129
32	612	410	758.9			16.66 ± 0.34	25.32 ± 1.06	20.26 ± 1.73	11.4 ± 1.2	1.22 ± 0.15
33	623	322	263.0	70	54	7.42 ± 0.24	23.98 ± 1.06	31.50 ± 1.37	41.7 ± 2.5	0.626 ± 0.070
34			495.8			11.46 ± 0.22	46.36 ± 2.59	30.99 ± 1.12	25.2 ± 1.2	0.704 ± 0.056
35		323	819.0			16.93 ± 0.26	71.28 ± 4.55	33.25 ± 1.16	18.0 ± 0.8	0.655 ± 0.048
36	633	519	419.4	49	47	11.32 ± 0.30	69.79 ± 4.72	40.30 ± 2.13	33.7 ± 2.3	0.543 ± 0.062
37	631	513	643.9			16.63 ± 0.34	101.12 ± 9.73	43.16 ± 2.23	24.0 ± 1.6	0.573 ± 0.057
38	634	528	787.8			25.00 ± 0.59	128.01 ± 21.63	48.39 ± 3.27	18.0 ± 1.5	0.669 ± 0.075
39	633	528	1026			24.96 ± 0.51	127.48 ± 25.71	38.86 ± 2.97	14.1 ± 1.4	0.690 ± 0.084
40	643	320	797.2	68	53	15.26 ± 0.49	111.4 ± 6.19	53.97 ± 2.74	33.7 ± 2.3	0.281 ± 0.032
41			893.0			17.69 ± 0.40	113.3 ± 4.53	57.53 ± 1.97	31.1 ± 1.4	0.283 ± 0.023
42			1097			20.31 ± 0.49	143.7 ± 9.14	59.52 ± 2.63	27.7 ± 1.6	0.272 ± 0.025
43	653	408	841.5	83	55	19.06 ± 0.41	172.0 ± 6.41	77.79 ± 2.60	39.8 ± 1.8	0.202 ± 0.018
44		410	1128			22.70 ± 0.61	201.7 ± 16.3	71.71 ± 3.70	30.0 ± 2.0	0.233 ± 0.025
45		408	1448			29.39 ± 0.59	298.6 ± 16.8	75.24 ± 2.87	23.7 ± 1.2	0.250 ± 0.020
46	663	321	1350	66	50	25.98 ± 0.72	333.4 ± 15.7	94.26 ± 4.05	34.7 ± 2.0	0.154 ± 0.016
47	662	322	1998			35.59 ± 0.87	467.5 ± 35.3	91.72 ± 4.63	23.8 ± 1.6	0.178 ± 0.018
48	673	508	1622	98	38	53.98 ± 2.93	1202 ± 136	180.6 ± 16.7	31.9 ± 3.8	0.144 ± 0.026

[a]The uncertainties represent one standard deviation.
[b]In units of molecules cm^{-3}.

$$K_c = k_f/k_r = (1 - x_{eq})/x_{eq}[C_2H_4]. \quad (28)$$

The equilibrium constant K_p (in units of atm^{-1}) was calculated from

$$K_p = K_c/RT = 7.34\times10^{21}\ K_c/T, \quad (29)$$

in which K_c is expressed in units of cm^3 molecule^{-1} and T in K. The values of x_{eq} and K_p derived from Eqs. (26)–(29) are also listed in Tables I and II. The condition $\alpha^2 \gg \beta$ can be verified from the values listed in Tables I and II; generally $\beta < 0.06\ \alpha^2$.

The error in the measurement of [OH] due to the error in the subtraction of the scattered light from the LIF signal is estimated to be ~2% of $[OH]_0$. If the entire [OH] temporal profile is shifted upward by 0.02 $[OH]_0$, the derived values of K_p decrease by ~6%. Uncertainty in the $[OH]_0$ measurement due to the instability of the LIF signal and the error in the timing of the two lasers is estimated to be approximately 3%. If the entire [OH] temporal profile is multiplied by 1.03, the derived values of K_p decrease by ~4%, respectively. The ~10 μs delay in the generation of OH after photolysis introduces ~2% error in the K_p values. The $[OH]_{eq}$ in Eq. (24) was overestimated because the equation ignored the period required for the equilibrium to be reached. The error in x_{eq} depends on λ_1 and it is typically less than 2%. The standard error of K_p values determined from the derived x_{eq} in the nonlinear fitting were typically ± 10%. The systematic errors in the measurements of temperature and $[C_2H_4]$ were about ± 2% and ± 5%, respectively. Therefore, the 95% confidence limits for the measurements of K_p are estimated to be approximately ± 25%.

A. The enthalpy and the entropy changes of $OH+C_2H_4 \rightarrow HOC_2H_4$

The van't Hoff plot K_p vs T^{-1} is shown in Fig. 2. As illustrated in the figure, the values of K_p obtained at high pressure (symbol □ for $513 < P < 616$ Torr) are within experimental uncertainties of those at low pressure (symbol ○ for $278 < P < 411$ Torr). The values of K_p are also independent of $[C_2H_4]$. The excellent linearity in Fig. 2 indicates that within experimental uncertainties, ΔH is independent of temperature; they were fitted well to the linear van't Hoff equation

$$\ln K_p = -(\Delta H/R)T^{-1} + \Delta S/R. \quad (30)$$

The fit yielded $\Delta H = -(30.3 \pm 0.5)$ kcal mol^{-1}; the uncertainties represent one standard deviation. The values of ΔS were then derived from ΔH and values of K_p for each experiment by using Eq. (30); an average of $\Delta S = -(30.9 \pm 0.3)$ cal K^{-1} mol^{-1} was obtained. Considering the errors in K_p and T, we report $\Delta H = -(30.3 \pm 0.8)$ kcal mol^{-1} and $\Delta S = -(30.9 \pm 1.0)$ cal K^{-1} mol^{-1} at $544 \leqslant T \leqslant 673$ K.

The values of ΔH and ΔS determined at high temperatures can be corrected to give ΔH^0 and ΔS^0 by means of statistical thermodynamics. On the basis of the structure and vibrational frequencies of HOC_2H_4 predicted by Sosa and Schlegel,[38,39] corrections of −0.4 kcal mol^{-1} and −0.5 cal K^{-1} mol^{-1} were derived for ΔH and ΔS, respectively, for the alternation of temperature from 600 to 298 K. The correction was not changed for ΔH, but decreased to −0.4 cal K^{-1} mol^{-1} for ΔS when the listed vibrational frequencies of HOC_2H_4 were decreased by 13%; the reduction ratio was determined by comparison of the observed vibrational frequencies of C_2H_4 with the theoretical prediction at the same level of sophistication as that for HOC_2H_4. *Thus, $\Delta H^0 = -(30.7 \pm 0.9)$ kcal mol^{-1} and $\Delta S^0 = -(31.3 \pm 1.1)$ cal K^{-1} mol^{-1}.*

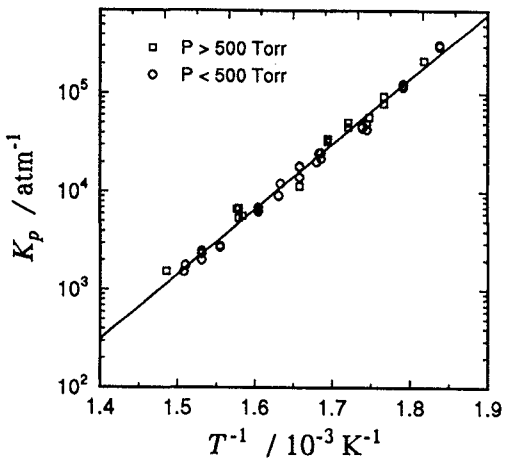

FIG. 2. A van't Hoff plot for the $OH + C_2H_4 \rightleftarrows^{M} HOC_2H_4$ equilibrium. □—$513 < P < 616$ Torr; ○—$278 < P < 411$ Torr.

To our knowledge, no experimental determination of ΔH and ΔS for the title reaction has been reported. Hinsta *et al.*[44] photodissociated a molecular beam containing 2-bromoethanol with 193 nm laser emission. They found that some HOC_2H_4 containing up to 43 kcal mol^{-1} of internal energy survived from further dissociation to $OH + C_2H_4$; the value was much greater than the expected HO–C_2H_4 bond energy. They proposed that the internal energy in HOC_2H_4 was probably mostly rotational and could not all be used to break the C–O bond, thus allowing the detection of metastable HOC_2H_4.

A few methods have been used to estimate ΔH^0 of reaction (12). Application of the additivity rule of Benson gave $\Delta H_f^0(HOC_2H_4) = -10.2$ kcal mol^{-1}; this result implies $\Delta H^0 = -32.1$ kcal mol^{-1}.[41] Assuming that the C–H bond strength in C_2H_5OH is ~95.1 kcal mol^{-1},[45] $\Delta H_f^0(HOC_2H_4) = -13.1$ kcal mol^{-1} was derived by using $\Delta H_f^0(H) = 52.1$, and $\Delta H_f^0(C_2H_5OH) = -56.1$ kcal mol^{-1},[46] hence $\Delta H^0 = -35.0$ kcal mol^{-1}. However, when the C–H bond strength of C_2H_6 100.7 ± 1.0 kcal mol^{-1} (Ref. 47) was used for that of H–C_2H_4OH, $\Delta H_0 = -29.5$ kcal mol^{-1} was derived instead. Although previous *ab initio* calculations yielded smaller values of $\Delta H \simeq -24$ kcal mol^{-1},[38,40] Sosa and Schlegel recently used a larger basis set and corrected their value of $\Delta H_f(HOC_2H_4)$ based on comparison of the theoretical calculation of the isodesmic reaction

$$C_2H_5 + CH_3OH \rightarrow HOC_2H_4 + CH_4, \quad (31)$$

with given experimental values of ΔH_f^0 for C_2H_5, CH_3OH, and CH_4; the corrected value yielded $\Delta H = -29$ kcal mol^{-1}.[39] The values derived from *ab initio* calculation represent $T = 0$ K; a correction of -1.1 kcal mol^{-1} should be employed to yield ΔH^0 at 298 K. Our experimental value $\Delta H^0 = -(30.7 \pm 0.9)$ kcal mol^{-1} is consistent with most of these estimates.

The entropy of HOC_2H_4 can be estimated from its structure and the vibrational frequencies predicted by theory. A value $S^0(HOC_2H_4) = 66.8$ cal K^{-1} mol^{-1} was calculated when the vibrational frequencies listed by Sosa and Schlegel[39] were used; the value decreased to 65.8 cal K^{-1} mol^{-1} when the vibrational frequencies were decreased by 13%. With $S^0(OH) = 43.9$ and $S^0(C_2H_4) = 52.4$ cal K^{-1} mol^{-1},[46] our experimental result of $\Delta S^0 = -(31.3 \pm 1.1)$ cal K^{-1} mol^{-1} yielded $S^0(HOC_2H_4) = 65.0 \pm 1.1$ cal K^{-1} mol^{-1}. Considering the possible uncertainties in the predicted structure and vibrational frequencies of HOC_2H_4, the agreement is excellent.

B. Assumptions in the derivation of the individual rate coefficients

To derive k_f, k_r, k_a, and k_{15} from the measured α, β, and γ by using Eqs. (20)–(22) requires certain assumptions or approximations. If one assumes that reaction (4), the H-abstraction channel, is negligible, the values k_{15} are approximated by k_8 which were determined by a fit of the [OH] temporal profiles recorded in the absence of C_2H_4; hence the values of k_f, k_r, and k_a were determined. This assumption is certainly valid at low temperature, but may not hold at temperatures above 600 K. Tables III and IV list the values of k_8 determined from experiments and the rate coefficients k_f, k_r, and k_a derived when $k_{15} = k_8$ was assumed. The corresponding values of K_p, derived from k_f/k_rRT, are also listed. The K_p values thus obtained are slightly greater, but within experimental uncertainties of those listed in Tables I and II which were derived from values of x_{eq}. A fit of K_p to Eq. (30) yielded $\Delta H = -(29.7 \pm 0.5)$ kcal mol^{-1} and $\Delta S = -(29.8 \pm 0.3)$ cal K^{-1} mol^{-1} within experimental uncertainties of those reported in the previous section.

If the rate expression for the H-atom abstraction channel reported by Tully[18]

$$k_4 = (3.36 \pm 0.64) \times 10^{-11} \exp[-(2997 \pm 144)/T] \times \text{cm}^3 \text{ molecule}^{-1} \text{ s}^{-1} \quad (32)$$

were used to derive k_{15} from Eq. (16), the k_a values determined by solving Eqs. (20)–(22) became negative for many experiments at higher temperature (nos. 32, 35, and 40–47 in Table II); therefore it is likely that Eq. (32) overestimated the rate coefficient k_4.

In order to estimate an upper limit of k_4, one could assume that the rate coefficient of the adduct loss k_a was

TABLE III. A summary of rate coefficients at $544 < T < 595$ K derived from various assumptions.

Expt. no.	T (K)	$[C_2H_4]$ (10^{13})[a]	k_8 (s^{-1})	Assuming $k_{15} = k_8$				Assuming $k_a = 40$ s^{-1}					Assuming Eq. (33) for k_4			
				k_a (s^{-1})	k_f[b]	k_r (s^{-1})	K_p (10^4 atm^{-1})	k_{15} (s^{-1})	k_4[c]	k_f[b]	k_r (s^{-1})	K_p (10^4 atm^{-1})	k_a (s^{-1})	k_f[b]	k_r (s^{-1})	K_p (10^4 atm^{-1})
1	544	23.5	22	40	3.21	132	32.70	22	0	3.15	133	31.92	39	3.19	133	32.27
2		36.8		42	3.48	152	30.99	37	0.41	3.43	153	30.26	40	3.49	152	30.83
3	550	37.8	20	73	3.50	201	23.21	206	4.92	3.00	234	17.11	71	3.49	202	22.92
4	558	29.8	68	71	2.81	296	12.47	150	2.75	2.51	327	10.10	68	2.78	298	12.27
5		52.4		74	3.02	317	12.51	222	2.94	2.74	351	10.28	71	3.00	320	12.31
6		100.7		71	3.10	351	11.61	314	2.49	2.84	381	9.81	67	3.07	353	11.44
7	566	47.7	20	125	2.85	415	8.88	250	4.82	2.35	500	6.11	120	2.82	419	8.72
8		75.0		110	3.38	439	9.98	363	4.57	2.93	509	7.47	105	3.36	443	9.83
9		93.1		113	3.30	434	9.86	460	4.73	2.83	507	7.24	108	3.27	437	9.67
10	573	40.5	20	132	2.57	587	5.60	160	3.46	2.25	679	4.25	124	2.54	594	5.48
11		73.4		122	2.69	644	5.35	244	3.05	2.40	726	4.23	114	2.67	651	5.25
12		107.1		111	3.14	676	5.97	340	2.99	2.85	747	4.90	104	3.12	682	5.86
13	575	126.6	100	123	1.69	464	4.66	425	2.57	1.43	547	3.34	113	1.67	472	4.50
14		163.3		122	1.85	493	4.78	528	2.62	1.59	575	3.52	112	1.82	501	4.63
15	573	169.2	86	141	1.62	460	4.50	580	2.92	1.33	562	3.03	131	1.59	469	4.34
16	575	236.2	100	144	1.86	517	4.60	837	3.12	1.56	621	3.20	134	1.84	526	4.46
17	581	66.2	20	190	3.02	733	5.21	360	5.14	2.51	882	3.60	181	2.99	741	5.10
18		101.3		176	3.36	780	5.43	524	4.98	2.87	916	3.96	167	3.33	788	5.34
19	590	79.1	20	233	3.16	1069	3.67	403	4.84	2.68	1262	2.64	220	3.13	1081	3.60
20		123.6		209	2.73	936	3.63	537	4.18	2.30	1105	2.60	196	2.70	948	3.54
21		165.1		194	2.87	957	3.73	677	3.98	2.47	1111	2.77	181	2.84	969	3.64
22	593	71.6	68	229	2.09	1031	2.51	299	3.23	1.76	1220	1.79	209	2.06	1050	2.43
23	595	101.5		196	2.19	1225	2.21	320	2.48	1.93	1381	1.72	175	2.16	1245	2.14
24	594	128.8		203	2.59	1215	2.63	465	3.08	2.28	1378	2.04	185	2.55	1232	2.56
25	593	192.9		180	2.59	1239	2.59	576	2.63	2.33	1379	2.09	162	2.56	1256	2.52

[a] In units of molecules cm^{-3}.
[b] In units of 10^{-12} cm^3 molecule^{-1} s^{-1}.
[c] In units of 10^{-13} cm^3 molecule^{-1} s^{-1}.

TABLE IV. A summary of rate coefficients at $603 < T < 673$ K derived from various assumptions.

Expt. no.	T (K)	$[C_2H_4]$ (10^{13})[a]	k_8 (s^{-1})	Assuming $k_{15}=k_8$				Assuming $k_a=40\ s^{-1}$					Assuming Eq. (33) for k_4			
				k_a (s^{-1})	k_f[b]	k_r (s^{-1})	K_p (10^4 atm^{-1})	k_{15} (s^{-1})	k_4[c]	k_f[b]	k_r (s^{-1})	K_p (10^4 atm^{-1})	k_a (s^{-1})	k_f[b]	k_r (s^{-1})	K_p (10^4 atm^{-1})
26	603	191.5	20	331	2.18	2 104	1.26	526	2.64	1.91	2395	0.969	291	2.14	2 143	1.22
27		99.9	36	345	2.19	1 222	2.18	472	4.36	1.75	1527	1.40	319	2.15	1 247	2.10
28		166.7		292	2.23	1 324	2.05	629	3.56	1.87	1576	1.44	266	2.19	1 349	1.97
29		251.3		280	1.75	1 372	1.55	690	2.60	1.49	1612	1.12	246	1.71	1 405	1.48
30		517.3		299	1.83	1 514	1.47	1414	2.66	1.56	1772	1.07	263	1.79	1 548	1.41
31	613	109.6	20	440	1.71	1 754	1.16	367	3.17	1.38	2154	0.768	389	1.67	1 804	1.11
32	612	758.9		171	1.93	1 855	1.24	980	1.26	1.80	1986	1.09	129	1.89	1 896	1.19
33	623	263.0	36	540	1.61	2 610	0.726	716	2.59	1.35	3110	0.512	454	1.57	2 695	0.685
34		495.8		544	1.68	2 555	0.774	1406	2.76	1.40	3059	0.540	463	1.63	2 635	0.731
35		819.0		517	1.66	2 808	0.695	2004	2.40	1.42	3285	0.508	429	1.61	2 895	0.656
36	633	419.4	60	932	1.72	3 098	0.645	1676	3.85	1.34	3990	0.389	820	1.68	3 209	0.606
37	631	643.9	50	807	1.90	3 508	0.631	2250	3.42	1.56	4276	0.425	701	1.86	3 614	0.598
38	634	787.8	80	618	2.55	4 220	0.699	2499	3.07	2.24	4799	0.541	526	2.50	4 312	0.672
39	633	1026		593	2.05	3 294	0.720	3095	2.94	1.75	3846	0.528	502	2.00	3 383	0.685
40	643	797.2	36	1114	1.23	4 283	0.328	2006	2.47	0.99	5357	0.210	885	1.18	4 511	0.299
41		893.0		935	1.33	4 818	0.316	1900	2.09	1.12	5713	0.225	708	1.28	5 044	0.290
42		1097		989	1.31	4 964	0.300	2334	2.09	1.10	5912	0.212	749	1.25	5 202	0.275
43	653	841.5	20	1514	1.34	6 266	0.240	2164	2.55	1.08	7739	0.157	1179	1.28	6 599	0.218
44		1128		1292	1.37	5 880	0.263	2714	2.41	1.13	7131	0.179	991	1.32	6 179	0.240
45		1448		1360	1.51	6 164	0.275	3873	2.66	1.24	7484	0.187	1073	1.45	6 450	0.253
46	663	1350	36	1998	1.22	7 428	0.182	3482	2.55	0.97	9386	0.114	1513	1.16	7 912	0.162
47	662	1998		1706	1.32	7 413	0.197	5004	2.49	1.07	9132	0.130	1326	1.26	7 845	0.178
48	673	1622	50	3325	2.21	14 740	0.164	6591	4.03	1.81	18020	0.109	2763	2.14	15 296	0.153
	E_a (kcal mol^{-1})			22.1[d]	−2.2[e]	23.2				−2.5[e]	23.9		20.6[d]	−2.3[e]	23.5	

[a] In units of molecules cm^{-3}.
[b] In units of 10^{-12} cm^3 $molecule^{-1}$ s^{-1}.
[c] In units of 10^{-13} cm^3 $molecule^{-1}$ s^{-1}.
[d] The value will increase by ~2.4 kcal mol^{-1} when the rate of diffusion of C_2H_4OH away from the probed volume (~20 s^{-1}) was subtracted from k_a.
[e] Derived from fitting the data with $P > 500$ Torr and $T < 590$ K.

small. The value $k_a = 40\ s^{-1}$ derived previously at 544 K (experiments 1 and 2) should be a realistic estimate of k_a because k_{15} was small at that temperature; it is also consistent with the rate of diffusion away from the detection region for the adduct. This value was used for all temperatures to solve k_{15}, k_f, and k_r by Eqs. (20)–(22). The results are also summarized in Tables III and IV. The values of K_p, calculated from the derived values of k_f and k_r, are also listed; they are approximately 25% smaller than those listed in Tables I and II and also showed greater variations, indicating that the assumption of a constant k_a was not adequate. Furthermore, the values of k_4 calculated from Eq. (16) with the derived k_{15} values are also listed in Tables III and IV. They do not correlate well with T^{-1} and are within the range $(2–5)\times10^{-13}$ cm^3 $molecule^{-1}$ s^{-1} for most experiments performed at $550 < T < 673$ K, inconsistent with a large activation energy expected for the abstraction reaction. However, a fit of K_p to Eq. (30) yielded $\Delta H = -(31.0 \pm 0.6)$ kcal mol^{-1} and $\Delta S = -(32.6 \pm 0.4)$ cal K^{-1} mol^{-1}, still close to our reported values; this result indicates that the ΔH and ΔS values are insensitive to the values of k_a and k_{15} under our experimental conditions.

A smaller value of k_4 derived from a calculation using the bond-energy-bond-order (BEBO) method was recommended by Tsang and Hampson,[48]

$$k_4 = 2.6\times10^{-20}\ T^{2.75}\exp(-2100/T) \times \text{cm}^3\ \text{molecule}^{-1}\ \text{s}^{-1}. \quad (33)$$

Equation (33) predicts the k_4 value of 6.87×10^{-14} cm^3 $molecule^{-1}$ s^{-1} at 673 K, approximately 17% of that predicted by Eq. (32). When the predicted values of k_4 were used to derive k_{15}, excellent results for k_f, k_r, k_a, and K_p were obtained, as also listed in Tables III and IV. The temperature dependence of K_p gave $\Delta H = -(30.2 \pm 0.5)$ kcal mol^{-1} and $\Delta S = -(30.8 \pm 0.3)$ cal K^{-1} mol^{-1} almost identical to the values reported in the previous section.

In conclusion, although accurate rate coefficients for the H-atom abstraction reaction could not be determined from our experiment, under our experimental conditions, the models which use a smaller rate coefficient for the H-atom abstraction reaction (Eq. 33) are preferred. At low temperatures, the derived rate coefficients are independent of the model because the H-abstraction channel is negligible in all cases.

C. The rate coefficients k_f and k_r

As listed in Tables III and IV, the rate coefficient of the reverse reaction k_r depends less on pressure than that of the forward reaction k_f. Figure 3 is the Arrhenius plot of k_r

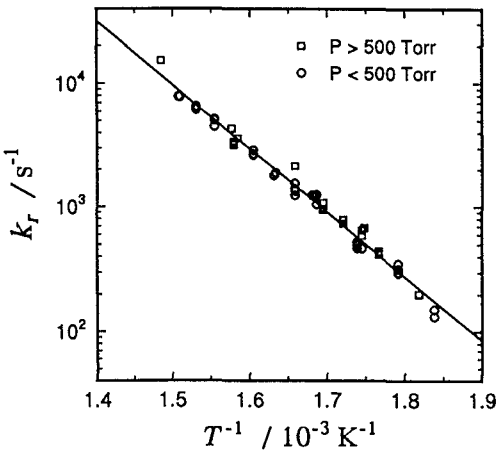

FIG. 3. An Arrhenius plot of k_r derived by using Eq. (33) for k_4. □—$513 < P < 616$ Torr; ○—$278 < P < 411$ Torr.

[derived by using Eq. (33) for k_4] with symbols □ for $513 < P < 616$ Torr and ○ for $278 < P < 411$ Torr. The least-squares fit of the entire set of data yielded an activation energy of 23.5 ± 0.4 kcal mol^{-1}, whereas the fit of only the data at $P > 500$ Torr gave $E_a = 23.7 \pm 0.8$ kcal mol^{-1}. The values of k_r derived with neglect of the H-atom abstraction reaction are slightly smaller than those shown in Fig. 3; the data at $P > 500$ Torr yielded $E_a = 23.5 \pm 0.8$ kcal mol^{-1}. The values of k_r derived with the assumption that $k_a = 40$ s^{-1} also yielded $E_a = 23.9 \pm 0.4$ kcal mol^{-1}; as before, these values are insensitive to the models employed. Hence, we report here

$$k_r = (6.2 \pm 1.0) \times 10^{11} \exp[-(11\,900 \pm 400)/T] \text{ s}^{-1}. \quad (34)$$

The uncertainties in k_f are greater than those in k_r. The Arrhenius plot of k_f is shown in Fig. 4 with symbols □ for $513 < P < 616$ Torr and ○ for $278 < P < 411$ Torr. Evidently at higher temperature, the high-pressure limit has not been reached even at $P = 400$ Torr. A least-squares fit of the data with $P > 500$ Torr yielded $E_a = -(3.9 \pm 0.7)$ kcal mol^{-1}. Values of $E_a = -(3.8 \pm 0.7)$ and $-(4.1 \pm 0.8)$ kcal mol^{-1} were derived from models with the assumption that $k_{15} = k_8$ and $k_a = 40$ s^{-1}, respectively. However, because at high temperature the k_f values are more sensitive to the values of k_a and k_{15} and their high-pressure limit requires higher pressure to reach, it is likely that the activation energy of $E_a = -(2.3 \pm 1.6)$ kcal mol^{-1} derived from fitting the data with $P > 500$ Torr and $T \leqslant 590$ K is more accurate. Therefore, we report

$$k_f = (4 \pm 3) \times 10^{-13} \exp[(1200 \pm 800)/T] \times \text{cm}^3 \text{ molecule}^{-1} \text{ s}^{-1}. \quad (35)$$

The activation energy is slightly greater than, but within experimental uncertainties of the 0.9 kcal mol^{-1} value reported in previous kinetic measurements at low temperature.

D. The rate coefficient k_a

The k_a values listed in Tables III and IV [assuming Eq. (33) for k_4] are plotted against T^{-1} in Fig. 5. All data except one [experiment (32)] showed an excellent linear correlation between ln k_a and T^{-1}. The large deviation of k_a in experiment (32) was due to a relatively small value of x_{eq} and a small kink in the slow component of the temporal profile of [OH]; hence this data point was not included in the least-squares fit. The activation energy was determined to be 20.6 ± 0.5 and 20.7 ± 0.8 kcal mol^{-1} when the entire data set and the data at $P > 500$ Torr were used, respectively.

In the model with $k_{15} = k_8$, the values of k_a at 673 K are approximately 30% greater than those shown in Fig. 5 because all the observed rate of loss was attributed to k_a. A value $E_a = 21.6 \pm 0.8$ kcal mol^{-1} was obtained from the

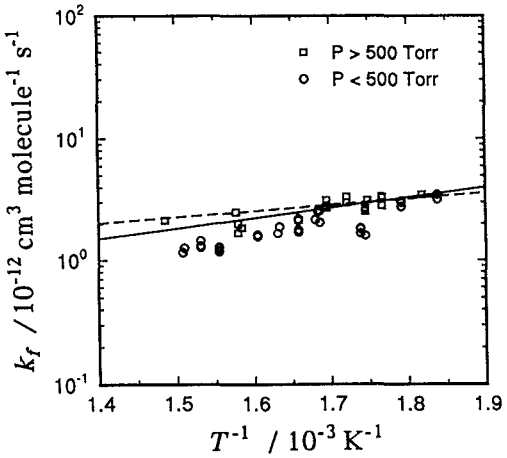

FIG. 4. An Arrhenius plot of k_f derived by using Eq. (33) for k_4. □—$513 < P < 616$ Torr; ○—$278 < P < 411$ Torr. The solid line represents the least-squares fit of the data with $P > 500$ Torr. The dashed line represents the least-squares fit of the data with $P > 500$ Torr and $T \leqslant 590$ K.

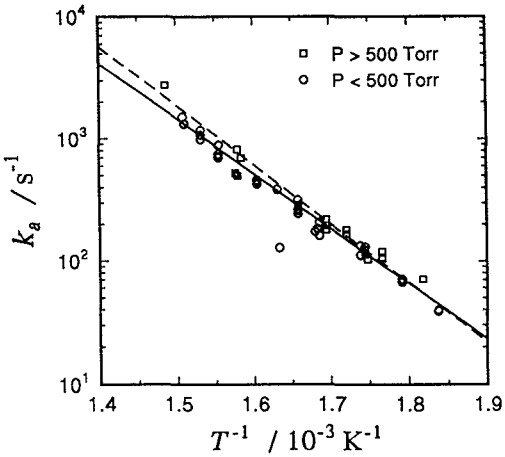

FIG. 5. An Arrhenius plot of k_a derived by using Eq. (33) for k_4. □—$513 < P < 616$ Torr; ○—$278 < P < 411$ Torr. The solid line represents the least-squares fit of the data [except for one point (see the text)]. The dashed line represents the least-squares fit of the data derived by neglecting the H-abstraction channel (data not shown).

data at $P > 500$ Torr. When the rate of diffusion of HOC_2H_4 away from the probed volume ($\sim 20\ s^{-1}$) was subtracted from k_a, an activation energy of (23.0 ± 0.7) kcal mol^{-1} was derived. Hence, we report

$$k_a = (8.8^{+25}_{-1.5}) \times 10^9 \exp[-(10\,400^{+1600}_{-400})/T]\ s^{-1}. \quad (36)$$

Sosa and Schlegel calculated various reaction potential surfaces of $OH + C_2H_4$ and the predicted barrier heights of 29, 32 and 34 kcal mol^{-1}, respectively, for the reverse reaction

$$HOC_2H_4 \xrightarrow{M} OH + C_2H_4, \quad (13r)$$

the [1,3]-hydrogen shift

$$HOC_2H_4 \rightarrow CH_3CH_2O, \quad (37)$$

and the β-hydrogen dissociation

$$HOC_2H_4 \rightarrow CH_2CHOH + H. \quad (38)$$

Although the predicted barriers for reactions (37) and (38) are higher than that of reaction (13), the tunneling effect of the H atom is expected to decrease substantially the activation energies of the former reactions. The tunneling effect in the similar reactions

$$OH + C_2H_2 \rightarrow HOC_2H_2 \rightarrow CH_2CO + H \quad (39)$$

$$\rightarrow CH_3 + CO \quad (40)$$

has been investigated theoretically by Miller and Melius.[49] Our E_a values of $(20.6^{+3.2}_{-0.8})$ and (23.7 ± 0.8) kcal mol^{-1} for k_a and k_r are consistent with this prediction, although we cannot specify which reaction path(s) is responsible for the loss of HOC_2H_4.

E. Simulation of the rate measurement at 673 K

Typically, in a rate measurement, a pseudo-first-order condition was employed and the logarithmic decay of the concentration of the reactant with respect to reaction time was followed. If a complex reaction mechanism is involved, the measurement is susceptible to interference, especially when the concentration of the reactant was probed within only a limited period of reaction.

In our experiments at high temperature, a large concentration of C_2H_4 ($\sim 10^{16}$ molecules cm^{-3}) was employed in order to obtain a distinctly double-exponential temporal profile of [OH] in the reaction period 50 μs–2 ms. In contrast, $[C_2H_4] \sim 10^{14}$ molecules cm^{-3} was used in a typical determination of the rate of the title reaction and [OH] was monitored in the later period of reaction, typically 1–20 ms. The small $[C_2H_4]$ used in the experiments implies a large value of x_{eq}; therefore only the slow component of the original double-exponential decay was observed under such experimental conditions.

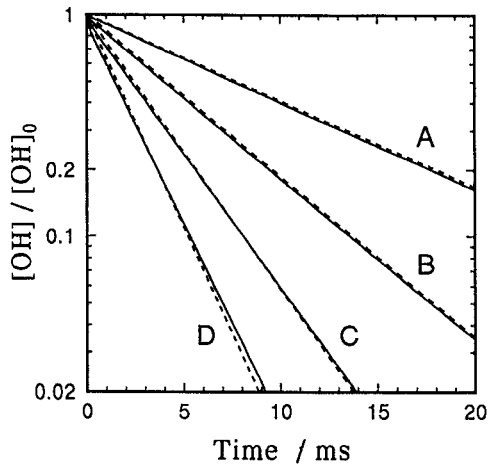

FIG. 6. A simulation of decay plots of [OH] at 508 Torr and 673 K. $[C_2H_4]$ (10^{14} molecules cm^{-3}) = (A) 1.0; (B) 3.0; (C) 6.0; (D) 10. The solid lines represent temporal profiles predicted by our model. The dashed lines represent pseudo-first-order decays predicted from Tully's data for k_4 [Eq. (32)]. The parameters are listed in Table V.

Under the condition $\alpha^2 \gg \beta$, the decay rate of the slow component of the [OH] temporal profile λ_1 is approximated by β/α. At small concentrations of C_2H_4, the value of α was dominated by $\gamma + k_{15}$. If the rate of the H-abstraction reaction is small, $\alpha \simeq \gamma$; hence

$$\lambda_1 \simeq \beta/\alpha \simeq k_8 + (k_f k_a/\gamma)[C_2H_4]. \quad (41)$$

Therefore, the dependence of the decay rate of the slow component on $[C_2H_4]$ yielded $k_f k_a/\gamma$. A value of $k_f k_a/\gamma = 4.07 \times 10^{-13}$ cm^3 molecule^{-1} s^{-1} was derived for $T = 673$ K and $P = 508$ Torr, this value is close to $k_4 = 3.91 \times 10^{-13}$ cm^3 molecule^{-1} s^{-1} derived from Tully's work.

With the rate coefficients k_f, k_r, and k_a determined at 673 K and 508 Torr in the model assuming $k_{15} = k_8$, the values α, β, λ_1, and λ_2 were calculated for each $[C_2H_4]$. Table V lists the values of α and β, the expression for the

TABLE V. Parameters for the simulation of decay rate at 673 K.

$[C_2H_4]$	From our mechanism with $k_{15} = k_8 = 50\ s^{-1}$			From Eq. (32)	
(10^{14})[a]	α (10^4 s^{-1})	β (10^6 s^{-1})	$[OH]/[OH]_0$	$k_4[C_2H_4]$ (s^{-1})	k_{15}[b] (s^{-1})
1.0	1.83	1.64	$0.990\exp(-90t) + 0.010\exp(-18246t)$	39	89
3.0	1.88	3.11	$0.970\exp(-167t) + 0.030\exp(-18611t)$	117	167
6.0	1.94	5.31	$0.942\exp(-277t) + 0.058\exp(-19164t)$	235	285
10.0	2.03	8.22	$0.905\exp(-413t) + 0.095\exp(-19912t)$	391	441

[a] In units of molecules cm^{-3}.
[b] $k_{15} = k_4[C_2H_4] + k_8$ with $k_8 = 50\ s^{-1}$.

temporal profile of [OH] [Eq. (23)], and the expected pseudo-first-order decay rate coefficient (k_{15}) using the values of k_4 reported by Tully[18] [Eq. (32)], for various concentrations of $[C_2H_4]$. The decay rates of the slow component of the double-exponential temporal profile are in excellent agreement with the anticipated pseudo-first-order decay rates, as demonstrated in Fig. 6. The solid lines are the predicted temporal profiles of [OH] based on the rate coefficients determined in this work, and the dashed lines are the predicted pseudo-first-order decays based on the reported k_4 by Tully. It is clear that the observed decay rates for the "abstraction channel" can also be simulated by our model which assumes a negligible rate for the abstraction of H. The model with low values of k_4 [Eq. (33)] also gave similar results.

IV. CONCLUSION

By analysis of the temporal profile of [OH] in the reaction of OH with C_2H_4, we determined the equilibrium constant of the title reaction. The temperature dependence of the equilibrium constant leads to $\Delta H^0 = -(30.7 \pm 0.9)$ kcal mol^{-1} and $\Delta S^0 = -(31.3 \pm 1.1)$ cal K^{-1} mol^{-1}. On the basis of analysis of the individual rate coefficients in the reaction mechanism, we think that previous studies may have overestimated the rate coefficient for the H-abstraction reaction near 673 K. The temperature dependence of the rate coefficients for the forward, the reverse, and the adduct-loss reactions have also been determined.

ACKNOWLEDGMENT

This research is supported by the National Science Council of the Republic of China (Contract No. NSC80-0208-M007-84).

[1] *Combustion Chemistry*, edited by W. C. Gardiner, Jr. (Springer, New York, 1984).
[2] D. J. Hucknall, *Chemistry of Hydrocarbon Combustion* (Chapman and Hall, New York, 1985).
[3] J. H. Seinfeld, *Atmospheric Chemistry and Physics of Air Pollution* (Wiley, New York, 1986).
[4] R. Atkinson, K. R. Darnall, A. C. Lloyd, A. M. Winer, and J. N. Pitts, Jr., Adv. Photochem. **11**, 375 (1979).
[5] A. D. Liu, W. A. Mulac, and C. D. Jonah, Int. J. Chem. Kinet. **19**, 25 (1987).
[6] N. R. Greiner, J. Chem. Phys. **53**, 1284 (1970).
[7] I. W. M. Smith and R. Zellner, J. Chem. Soc. Faraday Trans. **2**, 1617 (1973).
[8] F. Stuhl, Ber. Bunsenges. Phys. Chem. **77**, 674 (1973).
[9] D. D. Davis, S. Fischer, R. Schiff, R. T. Watson, and W. Bollinger, J. Chem. Phys. **63**, 1707 (1975).
[10] S. Gordon and W. A. Mulac, Int. J. Chem. Kinet. Symp. **1**, 289 (1975).
[11] A. C. Lloyd, K. R. Darnall, A. M. Winer, and J. N. Pitts, Jr., J. Phys. Chem. **80**, 789 (1976).
[12] R. Atkinson, R. A. Perry, and J. N. Pitts Jr., J. Chem. Phys. **66**, 1197 (1977).
[13] R. Overend and G. Paraskevopoulos, J. Chem. Phys. **67**, 674 (1977).
[14] (a) R. Atkinson, S. M. Aschmann, A. M. Winer, and J. N. Pitts, Jr., Int. J. Chem. Kinet. **14**, 507 (1982); (b) R. Atkinson and S. M. Aschmann, *ibid.* **16**, 1175 (1984).
[15] T. Klein, I. Barnes, K. H. Becker, E. H. Fink, and F. Zabel, J. Phys. Chem. **88**, 5020 (1984).
[16] R. Zellner and K. Lorenz, J. Phys. Chem. **88**, 984 (1984).
[17] V. Schmidt, G. Y. Zhu, K. H. Becker, and E. H. Fink, Bunsenges. Phys. Chem. **89**, 321 (1985).
[18] F. P. Tully, Chem. Phys. Lett. **96**, 148 (1983); **143**, 510 (1988).
[19] R. A. Cox and R. G. Derwent, Environ. Sci. Technol. **14**, 57 (1980).
[20] E. D. Morris, Jr., D. H. Stedman, and H. Niki, J. Am. Chem. Soc. **93**, 3570 (1971).
[21] J. N. Bradley, W. Hack, K. Hoyermann, and H. G. Wagner, J. Chem. Soc. Faraday Trans. **69**, 1889 (1973).
[22] A. V. Pastrana and R. W. Carr, Jr., J. Phys. Chem. **79**, 765 (1975).
[23] G. K. Farquharson and R. H. Smith, Aust. J. Chem. **33**, 1425 (1980).
[24] C. J. Howard, J. Chem. Phys. **65**, 4771 (1976).
[25] E. D. Morris, Jr., and H. Niki, J. Phys. Chem. **75**, 3640 (1971).
[26] J. N. Bradley, W. D. Capey, R. W. Fair, and D. K. Pritchard, Int. J. Chem. Kinet. **8**, 549 (1976).
[27] D. L. Singleton and R. J. Cvetonovic, J. Am. Chem. Soc. **98**, 6812 (1976).
[28] M. Mozurkewich and S. W. Benson, J. Phys. Chem. **88**, 6429, (1984); **88**, 6435 (1984).
[29] M. Bartels, K. Hoyermann, and R. Sievert, *19th International Symposium on Combustion* (The Combustion Institute, Pittsburgh, 1982), 61.
[30] C.-H. Kuo and Y.-P. Lee, J. Phys. Chem. **95**, 1253 (1991).
[31] R. Atkinson, J. Phys. Chem. Ref. Data, Monograph **1**, 82 (1989).
[32] W. B. DeMore, S. P. Sander, R. F. Hampson, M. J. Kurylo, D. M. Golden, C. J. Howard, and A. R. Ravishankara, and M. J. Molina, Evaluation Number 9, Publication 90-1, Jet Propulsion Laboratory, Pasadena, CA, 1990.
[33] D. L. Baulch, R. A. Cox, R. F. Hampson, Jr., J. A. Kerr, J. Troe, and R. T. Watson, J. Phys. Chem. Ref. Data **13**, 1310 (1984).
[34] R. Livington and H. Zeldes, J. Chem. Phys. **44**, 1245 (1966).
[35] H. Zeldes and R. Livingston, J. Chem. Phys. **45**, 1946 (1966).
[36] A. L. J. Beckwith and R. O. C. Norman, J. Chem. Soc. B, **1969**, 400.
[37] C. Anastasi, V. Simpson, J. Munk, and P. Pagsberg, J. Phys. Chem. **94**, 6327 (1990).
[38] C. Sosa and H. B. Schlegel, J. Am. Chem. Soc. **109**, 4193 (1987).
[39] C. Sosa and H. B. Schlegel, J. Am. Chem. Soc. **109**, 7007 (1987).
[40] C. F. Melius, J. S. Binkely, and M. L. Koszykowski, 8th International Symposium on Gas Kinetics, Nottingham, England, 1984.
[41] S. W. Benson, *Thermochemical Kinetics*, 2nd ed. (Wiley, New York, 1976).
[42] J. A. Kerr and M. J. Parsonage, *Evaluated Kinetic Data on Gas Phase Addition Reactions* (Butterworths, London, 1972).
[43] E. W.-G. Diau and Y.-P. Lee, J. Phys. Chem. **95**, 379 (1991).
[44] E. J. Hintsa, Z. Zhao, and Y.-T. Lee, J. Chem. Phys. **92**, 2280 (1990).
[45] B. L. Baulch, R. A. Cox, R. F. Hampson, Jr., J. A. Kerr, J. Troe, and R. T. Watson, J. Phys. Chem. Ref. Data **13**, 1376 (1984).
[46] M. W. Chase, Jr., C. A. Davies, J. R. Downey, Jr., D. J. Frurip, R. A. McDonald, and A. N. Syverud, JANAF Thermochemical Tables, 3rd ed., J. Phys. Chem. Ref. Data **14**, 1248 and 661 (1985).
[47] A. T. Castelhano, P. R. Marriot, and R. Griller, J. Am. Chem. Phys. **163**, 4262 (1981).
[48] W. Tsang and R. F. Hampson, Jr., J. Phys. Chem. Ref. Data **15**, 1189 (1986).
[49] J. A. Miller and C. F. Melius, 22nd Symposium (International) on Combustion 1031, 1988.